Magnetic Resonance Imaging 58 (2019) 6–13

Contents lists available at ScienceDirect

Magnetic Resonance Imaging

journal homepage: www.elsevier.com/locate/mri

Original contribution

NMR-based analysis of shear strength of weakly expansive clay in sodium chloride solution

Haihao Yu[a,*], De'an Sun[b], Huihui Tian[c]

[a] Laboratory of Geomechnics and Geotechnical Engineering, Guilin University of Technology, Guilin 541004, China
[b] Department of Civil Engineering, Shanghai University, Shanghai 200444, China
[c] State Key Laboratory of Geomechanics and Geotechnical Engineering, Institute of Rock and Soil Mechanics, Chinese Academy of Sciences, Wuhan, Hubei 430071, China

ARTICLE INFO

Keywords:
Nuclear magnetic resonance
Weakly expansive clay
Shear strength
NaCl solution

ABSTRACT

A series of direct shear and nuclear magnetic resonance (NMR) tests were performed on a compacted weakly expansive clay saturated by sodium chloride (NaCl) solutions with different concentrations to study the effect of NaCl solution on the shear strength and its mechanism. Results from the direct shear tests show that the shear strength decreases slightly with increasing the NaCl solution concentration when the concentration is less than 1.0 mol/L. The results of NMR tests show that the smaller transverse relaxation times (T_2) of specimens saturated by NaCl solutions with concentrations of 0.5 and 1.0 mol/L are less than that of the specimen saturated by deionized water. This means that the amount of smaller pores in the specimens saturated by deionized water is greater than that in specimens by NaCl solutions. That is, the specimen saturated by deionized water is denser than those by NaCl solutions under the same vertical pressure, and thus the shear strength of weakly expensive clay decreases with increasing the NaCl solution concentration.

1. Introduction

The inadequacy of the knowledge in chemo-mechanical property limits conventional soil mechanics applying to many fields including the storage of nuclear waste, oil wellbore stability, and soil stabilization, etc. It is becoming essential to investigate the chemo-mechanical coupling in clays. Most of geomaterials are composed of multiphases which are soil particles, pore solution, and air. The soil particles constituting the soil skeleton are electrically charged [24] because the negative charge exists on the particle surfaces, and it can adsorb polar hydrone and ions to form the diffuse double layers [3]. The pore fluid composition affects strongly the mechanical behavior of clayey soils, especially for expansive soils, in the practices of civil, energy and environmental engineering [10,29], because the properties of the pore fluid, which consist of solution concentration, dielectric constant and salt composition, can change the thickness of the diffuse double layers on the surface of clay particles [3]. The increasing electrolyte concentration or decreasing dielectric constant in the pore solution of clays results in a decrease in the thickness of the diffuse double layers [14].

Shear strength as an important mechanical parameter to the civil engineering is sensitive to the chemical composition of pore solution [20]. To obtain different chemical compositions of the pore solution, organics and inorganics, such as acetone, ethyl alcohol, NaCl, and potassium chloride, were widely used as solutes in the tests. The shear strength decreases with increasing the dielectric constant, which is mainly dominated by the organics in the pore solution [16]. The shear strength increases with increasing the electrolyte concentration, which is governed mainly by the inorganics in the pore solution [7,15].

In aforementioned studies, the shear strength could not be interpreted by the traditional effective stress because the chemical effect was neglected, while the traditional effective stress concept was modified to take into account the electrical attractive and repulsive forces [12,21]. Lambe [12] and Sridharan et al. [20] took the attractive and repulsive forces into consideration to describe the shear strength of clays, whereas Warkentin and Yong [28] considered that the interparticle repulsion force has impacted on the void ratio affecting the shear strength. Therefore, so far the knowledge about the contribution of the interparticle electrostatic forces to the shear strength is inconsistent.

Moreover, the shear strength is affected by the structure of plate-like particles [26,27]. The plate-like particles of clays are arranged: edge-face (E-F), edge-edge (E-E), and face-face (F-F) [25]. The type of three structures depends on the intergranular electrostatic forces [18]. In saturated clays, the distribution of pore solution can represent the pore characteristics in some extent. Nuclear magnetic resonance (NMR) can be used to determine the proton spin–spin relaxation time (T_2) distribution, which represents the local structure around the spin-bearing

* Corresponding author at: 12 Jiangan Road, Guilin 541004, China.
E-mail address: 2018094@glut.edu.cn (H. Yu).

https://doi.org/10.1016/j.mri.2019.01.002
Received 1 November 2018; Received in revised form 3 January 2019; Accepted 5 January 2019

molecule. There is a unique relation between T_2 and the pore size when the pore is full of water [5]. The NMR is a useful tool to investigate the distribution of water in clays [2,8,23].

The chemo-mechanical behavior of expansive clays is important in engineering practice, but most studies focus on strongly expansive clay. Many geotechnical engineering are constructed on weakly expansive clay, while the knowledge of chemo-mechanical behaviour of weakly expansive clays is limited. This paper aimed to investigate the chemo-mechanical behaviour of weakly expansive clays, especially the effect of the NaCl solution concentration on the shear strength and the distribution of water in the clays.

2. Test programe

A comprehensive laboratory programme was conducted with the aim of providing new test data about the effect of NaCl solution on the mechanical behavior of a weakly expansive clay. The programme involved the direct shear tests and NMR tests on weakly expansive clay saturated by NaCl solution with different concentrations.

2.1. Material and specimen preparation

The material tested is from Ningming area in Guangxi Autonomous Region, China. The mineral compositions of the weakly expansive soil are shown in Table 1. The soil is made up of four clay minerals, and the Illite-smectite mixed-layer mineral (I/S) is the mainly expansive mineral. Some physical-mechanical properties of the soil, such as specific gravity, liquid and plastic limits, maximum dry density, optimum water content, and free swelling ratio are summarized in Table 2. From the value of the free swelling ratio, the soil is classified as weakly expansive soil according to the Chinese National Standard Technical Code for Buildings in Expansive Soil Regions [13]. Fig. 1 shows the grading curve of Ningming expansive clay. The specimens were compacted statically to the targeted dry density of 1.6 g/cm^3. The NaCl solution with concentrations (n) of 0 (deionized water), 0.5, 1.0, and 2.0 mol/L were used to saturate compacted Ningming expansive clay specimens by the vacuum saturation under confined volume expansion for seven days. All the tests were performed at room temperature of about 20 °C.

2.2. Direct shear test

It is fact that the interparticle forces control the initial structure of clay, and the clay can generate the volume changes due to chemical and osmotic consolidations, which are induced by the changes in the ion concentration and osmotic pressure, respectively [14] when the clay with the pore solution of distilled water is immersed by saline solution. To exclude these effects, the soil specimens were made from the dry powder of clay sample. The initial water content of the soil sample was 0%. In this part, the powdered clay was dried at temperature of 105 °C for 12 h at least, and then the dry powdered clay was compacted to a ring specimen with the sizes of 15 mm thickness and 50 mm diameter. The water content of dry powdered clay increased only 0.12% after 1 h. The specimens were then saturated by the NaCl solution with different concentrations under confined volume expansion for seven days. After saturation, the specimen was installed in the direct shear box carefully. A small seating normal load was applied to the specimen, and the initial position was recorded. The vertical pressure was applied up to the target pressure step by step, and then the solution was poured into the shear box for keeping the specimens saturated. The vertical pressures for the direct shear tests were 100, 200, 300, and 400 kPa, respectively. In the direct shearing, a velocity of 0.005 mm/min in the horizontal direction was chosen for draining completely and no excess pore water pressure generates during shearing. Table 3 shows the void ratio (which is a ratio of pore volume to soil particle volume) of specimens at different stages for the direct shear tests. e_0 is an initial void ratio, e_s is the void ratio after saturation under constant volume, and e_c is the void ratio at different vertical pressures. e_0 is about 0.77, and e_s increases to about 0.79 after saturation during which specimens swelled slightly.

Table 1
Clay mineral of Ningming expansive clay.

I/S (%)	72.7
Illite (%)	8.3
Kaolinte (%)	14.6
Chlorite (%)	4.4

Table 2
Physico-chemical property of Ningming expansive clay.

Specific gravity	2.74
Liquid limit (%)	71.5
Plastic limit (%)	28.7
Maximum dry density (g/cm^3)	1.781
Optimum water content (%)	20.0
Free swelling ratio (%)	64.0
Cation exchange capacity (meq/100 g)	23.65

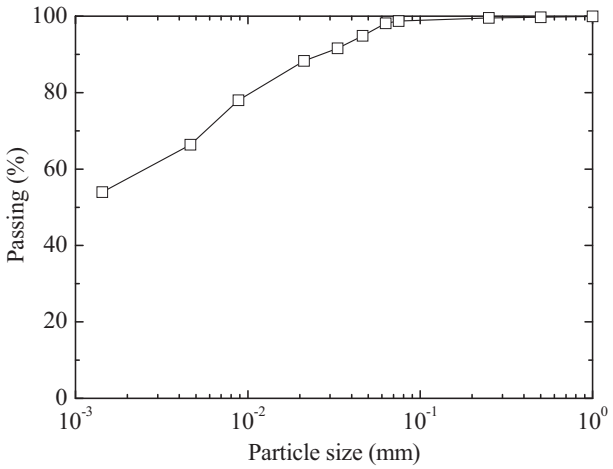

Fig. 1. Grading curve of Ningming expansive clay.

2.3. NMR test

According to Coates et al. [5], for a fluid saturated porous the NMR

Table 3
Void ratio of specimens for direct shear tests.

Vertical pressure (kPa)	n (mol/L)	e_0	e_s	e_c
100	0	0.776	0.797	0.719
	0.5	0.773	0.796	0.720
	1.0	0.778	0.803	0.724
	2.0	0.777	0.797	0.723
200	0	0.776	0.797	0.658
	0.5	0.778	0.799	0.663
	1.0	0.777	0.799	0.679
	2.0	0.771	0.791	0.679
300	0	0.778	0.801	0.635
	0.5	0.775	0.795	0.636
	1.0	0.774	0.795	0.637
	2.0	0.773	0.798	0.635
400	0	0.776	0.799	0.617
	0.5	0.774	0.794	0.619
	1.0	0.779	0.797	0.619
	2.0	0.777	0.798	0.618

Note: n is NaCl solution concentration, e_0 is an initial void ratio, e_s is the void ratio after saturation under constant volume, and e_c is the void ratio at different vertical pressures.

relaxation mechanisms are given by

$$\frac{1}{T_2} = \frac{1}{T_{2B}} + \frac{1}{T_{2S}} + \frac{1}{T_{2D}} \quad (1)$$

where T_2 is the transverse relaxation time of the pore fluid as measured by a CPMG sequence, T_{2B} is the transverse bulk fluid relaxation time, T_{2S} is the transverse surface relaxation time, and T_{2D} is the diffusion time and accounts for the transverse relaxation in an inhomogeneous magnetic field.

T_{2D} can be neglected compared to T_{2S}, if a short echo time is adopted [5]. Compared to T_{2S}, T_{2B} is very long ([5]; Saidian and Prasad 2015). Thus, at low field NMR, both T_{2B} and T_{2D} are negligible compared to T_{2S} [11]. In the fast diffusion limit, T_2 depends on T_{2S} and T_2 relaxation rate ($1/T_2$) is proportional to the surface-to-volume (S/V) ratio of the pore [4]. Hence, Eq. (1) is simplified as

$$\frac{1}{T_2} = \frac{1}{T_{2S}} = \rho_2 \left(\frac{S}{V}\right)_{\text{pore}} \quad (2)$$

where ρ_2 is the surface relaxivity coefficient, which is a characteristic parameter of magnetic interactions at the fluid-solid interface; $(S/V)_{\text{pore}}$ is the ratio of the pore surface area S to the pore water volume V, and is related to the pore size (d), i.e., $(S/V)_{\text{pore}} = F_s/d$. The geometry factor, F_s, depends on the pore shape, which is assumed to be a value of 2, 4 or 6 for planar, cylindrical or spherical pores, respectively. Because the tested soil particles with layered structures, the pore shape can be assumed planar, and then Eq. (2) becomes approximatively

$$\frac{1}{T_2} \approx \rho_2 \frac{2}{d} \quad (3)$$

where d is the pore size.

The NMR tests were performed on soil specimens saturated by NaCl solution with different concentrations or subsequently experiencing different consolidation pressures. After the saturation or saturation and consolidation, the specimens with the sizes of 20 mm thickness and 61.8 mm diameter were pushed out from the cutting ring for the specimen preparation or consolidation, and then were moved into a sample tube with the inner diameter of 110 mm for the NMR tests. The specimens were prepared in the same way to that for the shear tests, and were consolidated at the vertical pressures of 100, 200 and 400 kPa before being taken to complete the NMR tests. The free induction decay (FID) curves of the specimens were obtained. The FID curves of the soil specimens were determined by a MiniMR NMR setup with 12.58 MHz, which was jointly developed by the Institute of Rock and Soil Mechanics, Chinese Academy of Sciences, and Niumag Corporation, Suzhou, Jiangsu Province, China. The NMR setup consists of a sample tube, magnet unit, radio-frequency (RF) system and data acquisition-analysis system, which is sketched in Fig. 2. The magnetic field strength of magnet unit was 0.3 Tesla. To generate a stable and uniform main magnetic field, the temperature of the magnet unit is set to be 32 °C, within a variation of ± 01 °C. The used NMR setup has the receiver dead time of 35 μs. The CPMG for pulse sequence has the echo time of 0.2 ms and the repetition time is 1000 ms. 2000 echoes were used to obtain the FID curve of water for all specimens. The pulse length of 90° is 33 μs, and the pulse length of 180° is 65.04 μs. The value of T_2 was obtained by the simultaneous iterative reconstruction technique, and the iteration numbers was 10,000. The results were normalized by the mass of the NMR specimens.

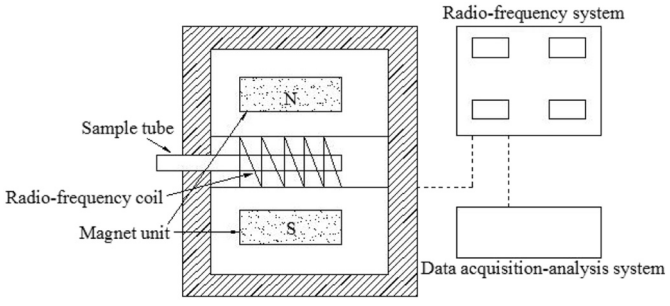

Fig. 2. The schematic map of MiniMR NMR.

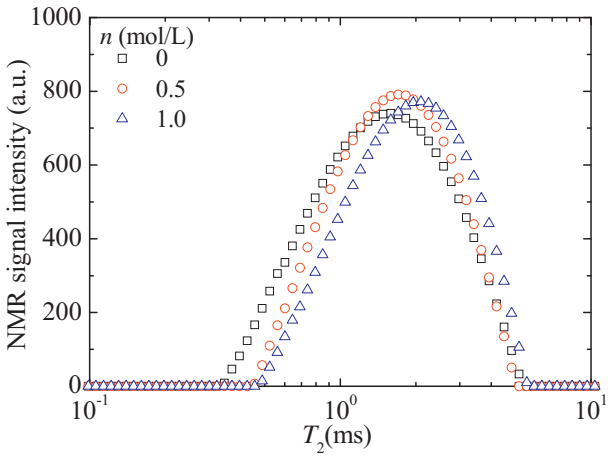

Fig. 3. T_2 distribution curves of expansive clay specimens saturated by NaCl solution with different concentrations.

3. Results and discussion

3.1. Results of NMR test

Fig. 3 shows the results of the NMR tests performed on the expansive clay specimens saturated by NaCl solution with different concentrations. It can be seen that T_2 of the specimens saturated by 0, 0.5 and 1.0 mol/L NaCl solution span from 0.34 to 5.17 ms, 0.45 to 4.8 ms and 0.48 to 5.5 ms, respectively. And T_2 at peak increases with increasing the NaCl solution concentration, and are 1.59, 1.70 and 2.10 ms for the concentrations of 0, 0.5 and 1.0 mol/L. The smallest value of T_2 increases with the solution concentration. From Eq. (3), the pore size of the specimen saturated by 0 mol/L solution is smaller than that of the specimens by 0.5 and 1.0 mol/L solutions.

Fig. 4 shows the sketch of the structural arrangements of compacted clay [6], which is considered to be the soil structure of compacted weakly expansive clay used in this paper. The pore in the elementary particle in Fig. 4 is a microscopic level [9]. During saturation, these

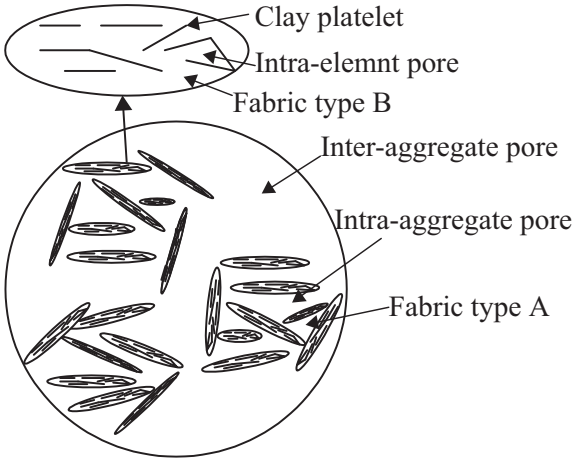

Fig. 4. Fabric type A is microfabric of clay predominantly made up of aggregations of elementary particle arrangements, and fabric type B is elementary particle arrangement in a parallel configuration.

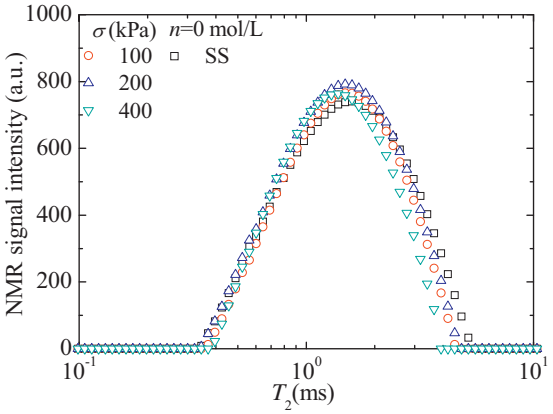

(a) n=0 mol/L

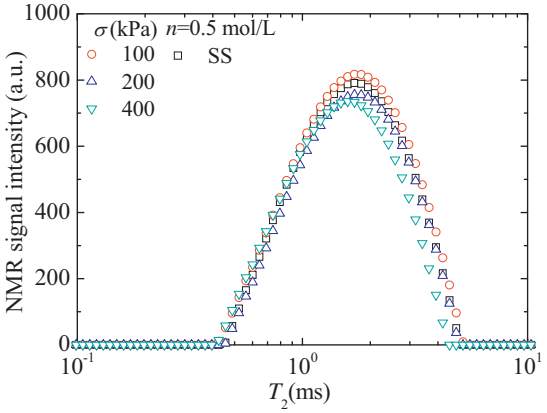

(b) n=0.5 mol/L

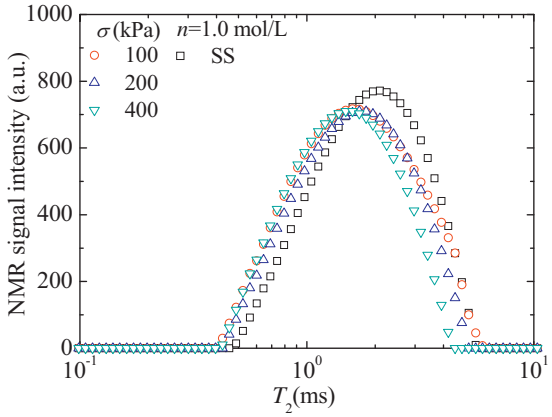

(c) n=1.0 mol/L

Fig. 5. T_2 distribution curves of saturated specimens with the same NaCl solution concentration at different vertical pressures.

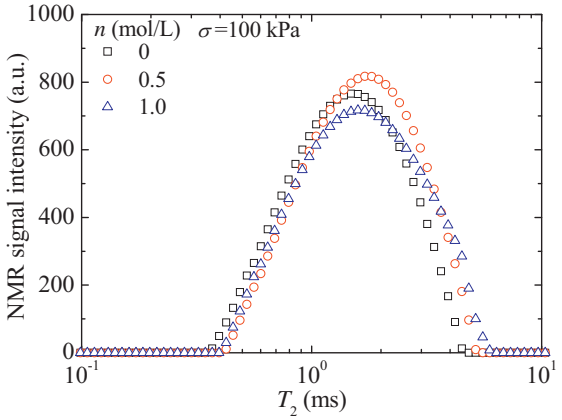

(a) σ=100 kPa

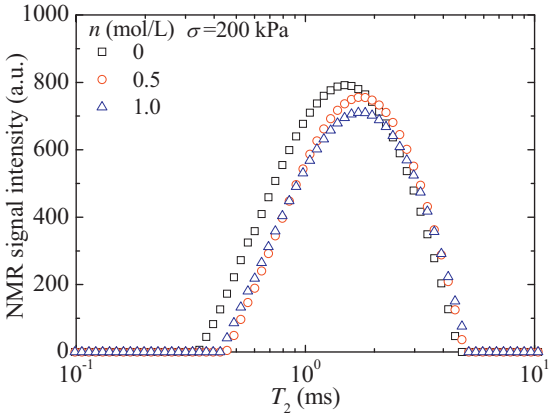

(b) σ=200 kPa

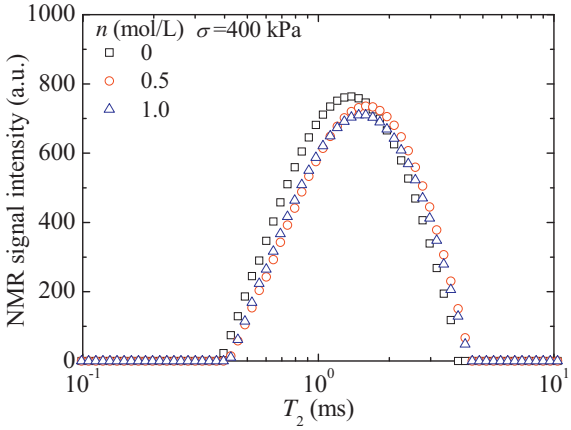

(c) σ=400 kPa

Fig. 6. T_2 distribution curves of specimens saturated by NaCl solution with different concentrations at the same vertical pressure.

specimens were limited under constant volume, and the microstructural pores swell to fill in the macrostructural pores. The swelling potential of the soils in deionized water (0 mol/L) is higher than that in NaCl solution [17]. As the concentration increases, the swelling potential decreases. Thus the macrostructural pore are filled more sufficient with deionized water than in NaCl solution, and the mean pore size of the specimen saturated by 0 mol/L solution is smaller than that of the specimens by 0.5 and 1.0 mol/L solutions.

Fig. 5 shows the NMR test results of the specimens saturated by NaCl solution with the same concentrations under different consolidation pressures. In the figure, "SS" means saturated specimen, for which no consolidation pressure was applied. Inspection of Fig. 5 indicates that the scope of T_2 decreases with the increase in the vertical pressure, and that the T_2 distribution curve shifts down somewhat with increasing the concentration and pressure, particularly for 1.0 mol/L. The NMR test results of the specimens saturated by NaCl solution with different concentrations at the same consolidation pressure are shown in Fig. 6. Under the same vertical pressure, the mean pore size of the

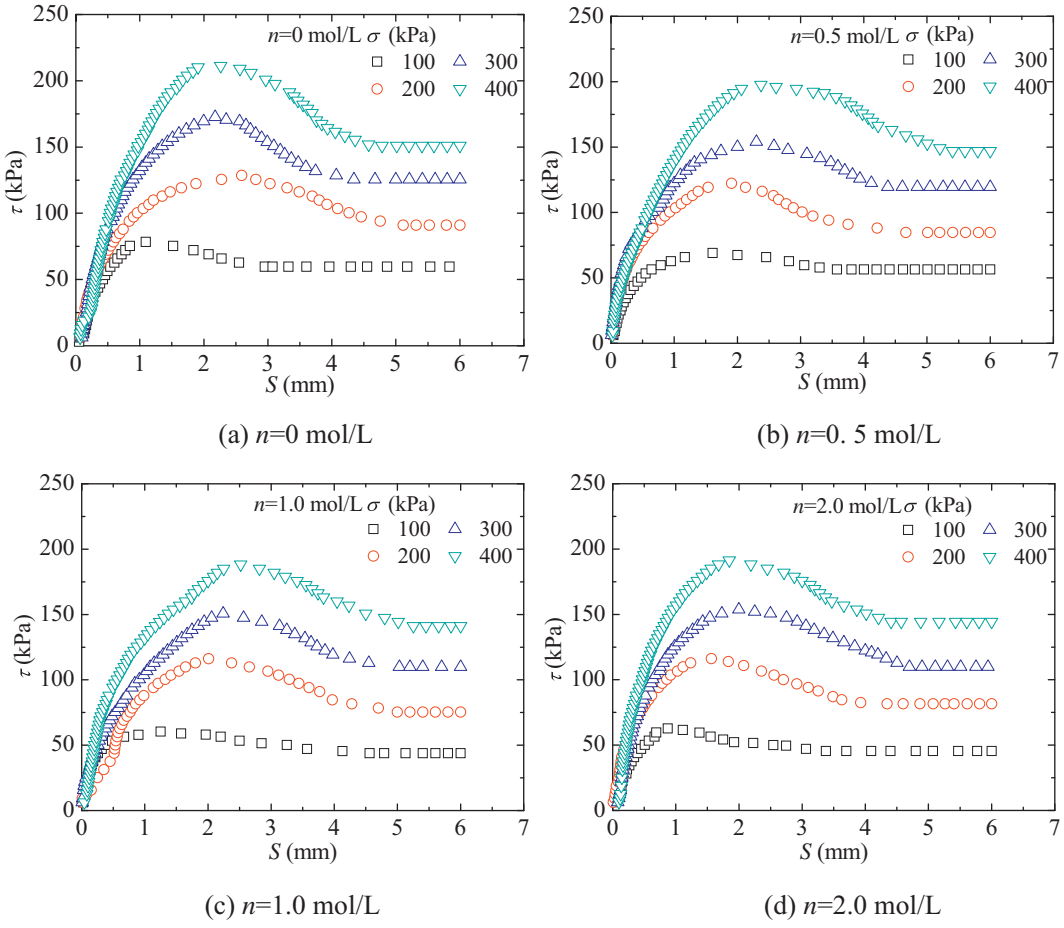

Fig. 7. Shear stress vs. shear displacement relation of Ningming expansive clay saturated by NaCl solution with different concentrations.

specimen saturated by 0 mol/L solution is also smaller than that of the specimens by 0.5 and 1.0 mol/L solutions.

3.2. Effect of pore solution concentration on shear strength

Fig. 7 shows results of the direct shear tests, which are in terms of shear displacement (S) against shear stress (τ) under different vertical pressures (σ). It is observed that there is a peak value of the shear stress for all concentrations, and a stable value of τ for large S. The peak and stable shear stresses are taken as the peak shear strength and residual shear strength, respectively.

The relation between shear strength and normal stress can be expressed by the Mohr-Coulomb equation:

$$\tau_f = c + \sigma \tan\varphi \quad (4)$$

where τ_f is the shear strength at peak or residual, c is an cohesion intercept, φ is an friction angle. Fig. 8 shows results of the direct shear tests, expressed by the vertical pressure against peak shear strength or residual shear strength. It can be seen that there is a linear relation for a given NaCl solution concentration. The parameters of linear fitting analysis are shown in Table 4.

Fig. 9 shows the shear strength of the weakly expansive clay saturated by NaCl solution with different concentrations. Fig. 9(a) shows the peak shear strength against the pore solution concentration at different vertical pressures. At the vertical pressure of 100 kPa, the peak shear strength decreases slightly with increasing the pore solution concentration when the concentration is less than 1.0 mol/L, while the variation in the peak shear strength at the concentrations of 1.0 and 2.0 mol/L is insignificant. At the vertical pressures of 200, 300 and 400 kPa, the variation in the peak shear strength is similar to that at the vertical pressures of 100 kPa.

Fig. 9(b) shows the residual shear strength against the pore solution concentration at different vertical pressures. The residual shear strength also decreases with increasing the pore solution concentration for the concentration less than 1.0 mol/L, and the residual shear strength in 2.0 mol/L NaCl solution is close to that in 1.0 mol/L solution.

Fig. 10 shows the shear strength parameters of the weakly expansive clay saturated by NaCl solution with different concentrations. Fig. 10(a) shows the cohesion against the pore solution concentration. It can be seen that the cohesions at peak and residual decrease with increasing the concentration of pore solution for the concentration less than 1.0 mol/L. The cohesion in 1.0 mol/L NaCl solution is almost the same as that in 2.0 mol/L NaCl solution. Fig. 10(b) shows that the friction angle of peak shear strength decreases slightly with increasing the concentration, but the variation in the friction angle of residual shear strength is negligible for different concentrations.

During the direct shear tests, the particles around the shear surface depart from the initial position. This movement of clay particles which depart from the initial position is hindered by the adjacent particles. The inhibition of interparticles produces the shear strength at macroscope. The whole shear process consists of three stages, as shown in Fig. 11. The inhibition of interparticles induced from the physic-chemical forces between clay particles, the viscous damping of adsorbed water at the surface of clay particles, and mechanical locking between interparticles [12]. In the different shear stages, the ways of inhibition of interparticles are different.

At the initial stage of the shearing, there is a potential shear surface. The shear surface is formed not by breaking the particle, but driving the particles apart their position. In Fig. 12, Particle **a** is located on a potential shear surface. To form shear surface in the process of shearing,

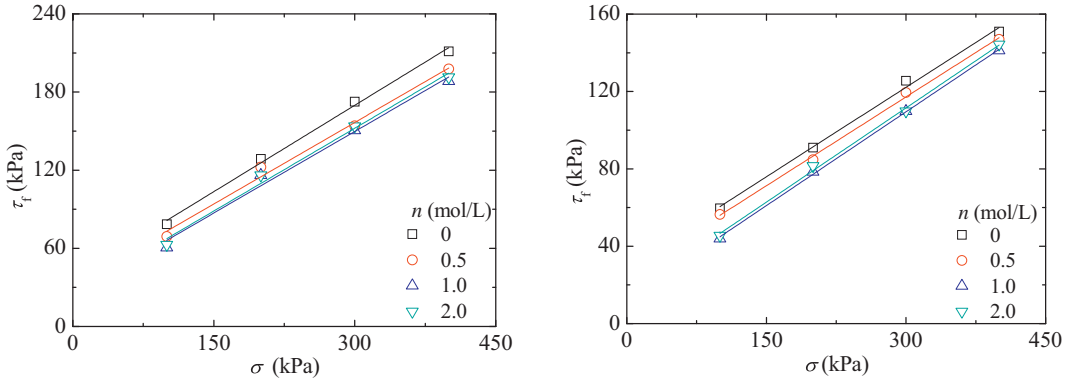

(a) Peak shear strength (b) Residual shear strength

Fig. 8. Shear strength vs. vertical stress relation.

Table 4
Parameter of linear fitting analysis.

Concentration (mol/L)	Strength type	Cohesion (kPa)	Friction angle (degree)	R-square
Deionized water	Peak shear	37.15	23.9	0.99
	Residual shear	29.61	17.2	1.00
0.5	Peak shear	31.38	22.7	0.99
	Residual shear	25.36	17.1	1.00
1.0	Peak shear	24.39	22.7	0.98
	Residual shear	12.55	18.0	1.00
2.0	Peak shear	25.10	23.0	0.99
	Residual shear	14.12	17.8	1.00

Particle **a** must be kept away its primary position to a new position. During moving, Particle **a** is subjected to the resistances from other particles in Aggregate **C**. All the aggregates around the potential shear surface are in similar process. At the stageI, the main ways of inhibition are the physic-chemical forces and mechanical locking between particles in the aggregates. The physic-chemical forces between interparticles, either the Van der Waal attractive force or diffuse double layer repulsive force, hinder the particle from the movement.

Along with the shearing, the mechanical locking between particles in the aggregates becomes more and more intense. In the meantime the viscous damping of the adsorbed water at the surface of clay particles starts to work. With increasing the shear stress, the soil is at the stageII where the mechanical locking occurs between aggregates. As shown in Fig. 11, Aggregate **C** and Aggregate **D** hinder each other moving in the process of shearing. At the stageII, all inhibitions among particles and/or aggregates reach the most intense, and thus the shear stress reaches the maximum. After the maximum shear stress, the particles around the shear surface tend to parallel to the shear surface, and thus the mechanical locking may disappear, while the aggregates around the shear surface are destroyed.

In the last, the soil is at the stage III, at which the sketch of microstructure is shown in Fig. 13. Around the shear surface, the particles become to the oriented arrangements, which formed a shear zone. At the stage III, there is the physic-chemical forces between particles and the viscous damping of the adsorbed water at the surface of clay particles but no mechanical locking.

In Fig. 10(b), it can be seen that the peak friction angle is larger than that at the residual. The friction angle is a macroscopic result of the viscous damping of the adsorbed water at the surface of clay particles and mechanical locking among particles and/or aggregates. In the procedure of the shear test, the mutual inhibition effects among particles and/or aggregates are most strongly at the peak shear stress. In the last shear stage, the particles around the shear surface are oriented which are parallel to the shear surface [22], and the mechanical locking exists hardly. Therefore, the friction angle of the peak shear strength is larger than that of the residual shear strength.

NaCl solution can restrains the diffuse double layers thickness. The decrease in the diffuse double layers thickness can result in the decrease in the viscous damping of the adsorbed water at the surface of clay particles [19], which results in the decrease in frictional strength. Fig. 14 shows the results of relative diffuse double layers thickness changing with increasing the pore solution concentration by Eq. (5) [14]:

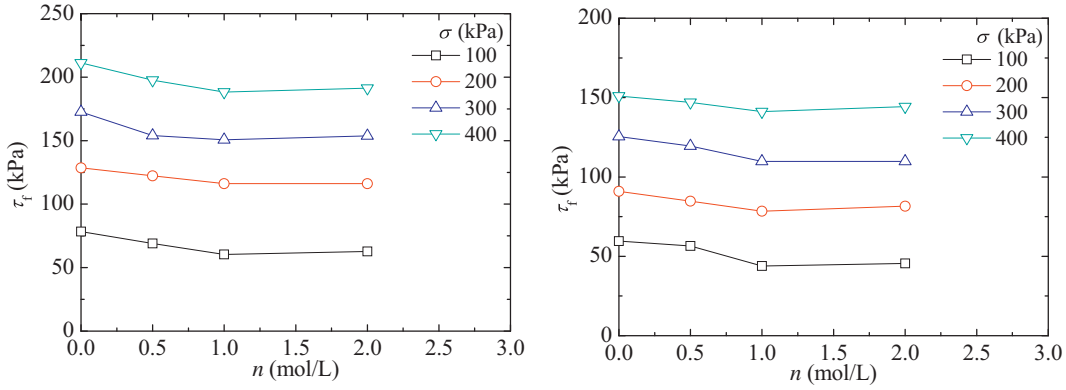

(a) Peak shear strength (b) Residual shear strength

Fig. 9. Shear strength vs. NaCl solution concentration relation.

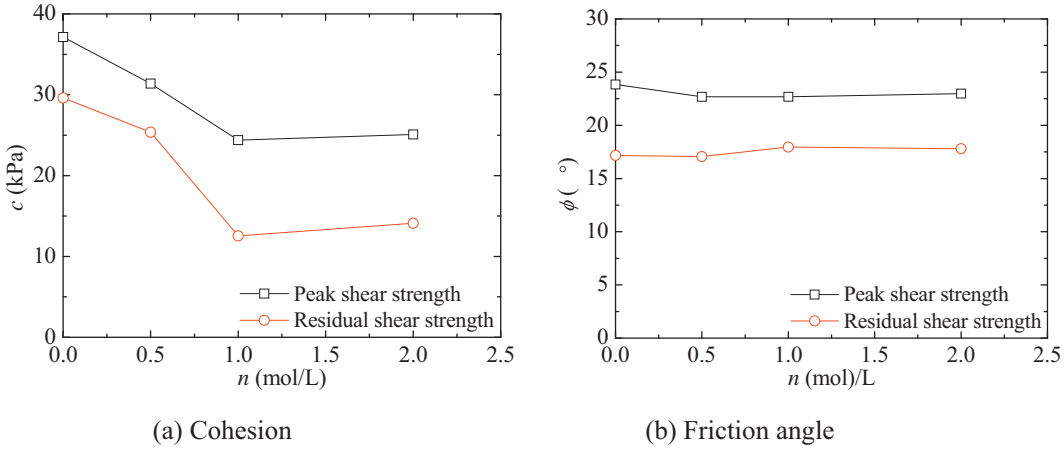

Fig. 10. Shear strength parameters vs. NaCl solution concentration relation.

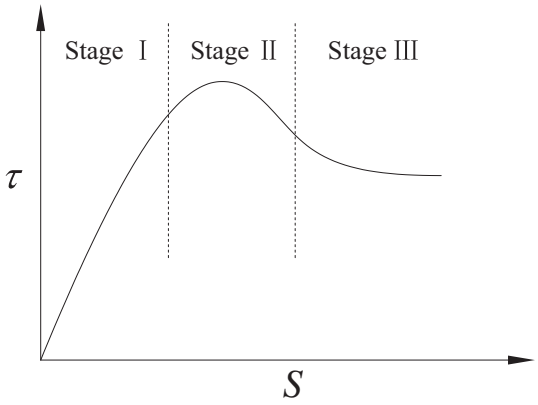

Fig. 11. Shear stress vs. shear displacement relation.

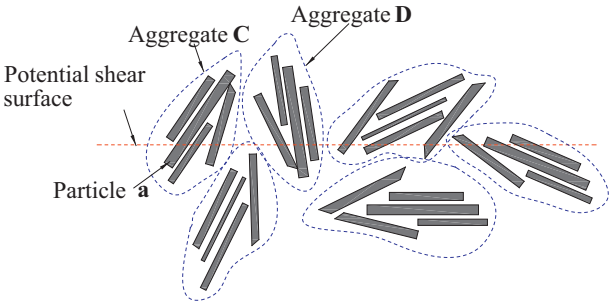

Fig. 12. Sketch of soil microstructure in shearing.

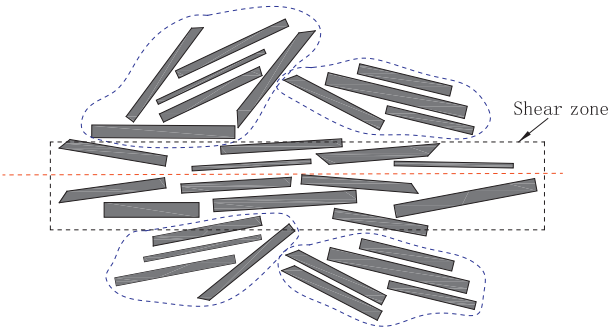

Fig. 13. Sketch of soil microstructure after direct shear test.

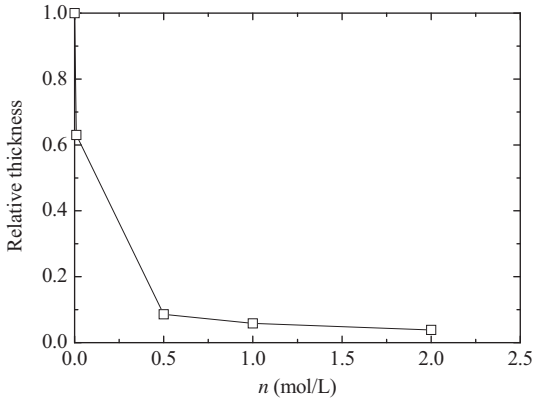

Fig. 14. Relative thickness of diffuse double layers at different concentrations.

$$\frac{1}{K} = \left(\frac{\varepsilon_0 DkT}{2n_0 e^2 v^2}\right)^{1/2} \quad (5)$$

where $1/K$ is the thickness of diffuse double layers thickness, ε_0 is the permittivity of vacuum, D is the dielectricconstant of the medium, k is Boltzmann's constant, T is the absolute temperature in Kelvin, n_0 is the electrolyte concentration, e is elementary charge, and v is cation valence. The diffuse double layers thickness of specimens in deionized water was defined as unit thickness. The relative thickness reduces rapidly as the concentration is smaller than 1.0 mol/L. When the concentration is greater than 1.0 mol/L, the relative thickness reduces slightly. Otherwise, the macrostructural pores are filled more sufficient with deionized water than in NaCl solution. The inhibition of interparticles is strong in the specimen saturated by 0 mol/L NaCl solution, and thus the strength is the biggest.

4. Conclusions

A series of direct shear and NMR tests were performed on compacted weakly expansive clay to investigate the effect of NaCl solution on the mechanical behavior of weakly expansive clay. The following conclusions can be obtained from this study:

(1) The results of NMR tests show that the smallest value of T_2 increases with the solution concentration. When the specimens are saturated by deionized water, and then were taken to be consolidated, the smallest value of T_2 also increases with the solution concentration at the same vertical pressure. The mean pore size of the expansive clay specimen saturated by deionized water is smaller than that of the specimens saturated by NaCl solutions with 0.5 and 1.0 mol/L

under limited volume expansion.

(2) When the NaCl solution concentration is less than 1.0 mol/L, the shear strength decreases with increasing the concentration. But when the concentration is greater than 1.0 mol/L, the variations in the diffuse double layers thickness is negligible, and thus the shear strength at 2.0 mol/L is close to that at 1.0 mol/L. According to the results of NMR tests, the NaCl solution increases the mean pore size, which results in the decrease in the inhibition of interparticles, and thus the shear strength decreases.

(3) The cohesions at peak and residual and the friction angle at peak all decrease with increasing the NaCl solution concentration, while the variation in the friction angle at residual is negligible for different concentrations.

Acknowledgements

The authors express their gratitude for the grants provided by the National Natural Science Foundation of China (No. 11672172 and 41502301). We appreciate Guangxi Key Laboratory of New Energy and Building Energy Saving (Guilin University of Technology), for supplying the NMR testing instrument through the opening fund (No. 17-J-22-1).

References

[2] Black PB, Tice AR. Comparison of soil freezing curve and soil curve data for Windsor sandy loam. Water Resour Res 1989;25:2205–10.
[3] Bolt GH. Analysis of the validity of the Gouy-Chapman theory of the electric double layer. J Colloid Sci 1955;10(2):206–18.
[4] Brownstein KR, Tarr CE. Importance of classical diffusion in NMR studies of water in biological cells. Phys Rev 1979;19(6):2446–53.
[5] Coates GR, Xiao LL, Prammer MG. NMR logging principles and application. Houston: Halliburton Energy Services Publication1999.
[6] Croney D, Coleman JD, Black WPM. Studies of the movement and distribution of water in relation to highway design and performance. Highway research board special report. 40. 1958. p. 226–52.
[7] Di Maio C, Fenelli GB. Residual strength of kaolin and bentonite: the influence of their constituent pore fluid. Geotechnique 1994;44(4):217–26.
[8] Dvinskikh SV, Sztkowski K, Furo I. MRI profiles over very wide concentration ranges: application to swelling of a bentonite clay. J Magn Reson 2009;198(2):146–50.
[9] Gens A, Alonso EE. A framework for the behaviour of unsaturated expansive clays. Can Geotech J 1992;29(6):1013–32.
[10] Homand S, Shao JF. Mechanical behavior of a porous chalk and water/chalk interaction. Part I: experimental study. Oil Gas Sci Technol 2000;55(6):591–8. (Revue d IFP Energies nouvelles).
[11] Kleinberg RL. Nuclear magnetic resonance pore-scale investigation of permafrost and gas hydrate sediments. In: Rothwell RG, editor. New techniques in sediment core analysis. Geological Society, London, Special Publications, 267. 2006. p. 179–92.
[12] Lambe TW. A mechanistic picture of shear strength in clay. Proceeding of research conference on shear strength of cohesive soils. Boulder, Colorado: ASCE; 1960. p. 555–80.
[13] Ministry of Housing and Urban-Rural Development of the People's Republic of China. Technical code for buildings in expansive soil regions. GBJ50112–2013. Beijing: China Architecture and Building Press; 2013.
[14] Mitchell JK, Soga K. Fundamentals of soil behavior. New York: Wiley; 2005.
[15] Moore R. The chemical and mineralogical controls upon the residual strength of pure and natural clays. Geotechnique 1991;41(1):35–47.
[16] Moore CA, Mitchell JK. Electromagnetic forces and soil strength. Geotechnique 1974;24(4):627–40.
[17] Rao SM, Thyagaraj T, Rao PR. Crystalline and osmotic swelling of an expansive clay inundated with sodium chloride solutions. Geotech Geol Eng 2013;31(4):1399–404.
[18] Sides G, Barden L. The microstructure of dispersed and flocculated samples of kaolinite, illite, and montmorillonite. Can Geotech J 1970;8(3):391–9.
[19] Sridharan A. Di Maio C, Hueckel T, Loret B, editors. Engineering behavior of clays: influence of mineralogy. Chemo-mechanical coupling in clays: from nano-scale to engineering applications. The Netherlands: A.A. Balkema Publishers; 2002. p. 3–28.
[20] Sridharan A, Rao SN, Rao GV. Shear strength characteristics of saturated montmorillonite and kaolinite clays. Soils Found 1971;11(3):1–22.
[21] Sridharan A, Rao GV. Mechanisms controlling the volume change behaviour of saturated clays and the role of the effective stress concept. Geotechnique 1973;23(3):359–82.
[22] Tchalenko JS. Similarities between shear zone of different magnitudes. Geol Soc Am Bull 1970;81:1625–40.
[23] Tian HH, Wei CF, Wei HZ, et al. An NMR-based analysis of soil-water characteristics. Appl Magn Reson 2014;45(1):49–61.
[24] van Olphen H. Forces between suspended bentonite particles. Clay Clay Miner 1956;4:204–24.
[25] van Olphen H. Internal mutual flocculation in clay suspension. J Colloid Sci 1964;19(4):313–22.
[26] Wang YH, Siu WK. Structure characteristics and mechanical properties of kaolinite soils. I. Surface charges and structural characterizations. Can Geotech J 2006;43(6):587–600.
[27] Wang YH, Siu WK. Structure characteristics and mechanical properties of kaolinite soils. II. Effects of structure on mechanical properties. Can Geotech J 2006;43(6):601–17.
[28] Warkentin BP, Yong RN. Shear strength of montmorillonite and kaolinite related interparticle forces. Clay Clay Miner 1962;9:210–8.
[29] Xu YF, Xiang GS, Jiang H, et al. Role of osmotic suction in volume change of clays in salt solution. Appl Clay Sci 2014;101:354–61.